Synthesis of Novel Nanostructures by Metal−Polytetrafluoroethene Thermolysis

Andrzej Huczko,*,† Hubert Lange,† Grzegorz Chojecki,† Stanisław Cudziło,‡ Yan Qiu Zhu,§ Harold W. Kroto,§ and David R. M. Walton§

Department of Chemistry, Warsaw University, 02-093 Warsaw, Poland, Faculty of Armament and Aviation Technology, Military University of Technology, 00-908 Warsaw, Poland, and School of Chemistry, Physics and Environmental Science, University of Sussex, Brighton BN1 9QJ, United Kingdom

Received: October 4, 2002

Novel ceramic and carbon nanostructures have been created by thermolysis of mixtures containing polytetrafluoroethene (PTFE) and a pure metal or metal alloy in a calorimetric bomb. The influence of the stoichiometry was studied for Si-containing reactants for which the yield of the nanofibers was the highest. The process was monitored by measuring the heat of reaction and by differential thermal analysis/thermogravimetric techniques. The reaction temperatures were measured, and the heating rates of the reactants during thermal wave propagation were estimated. Elemental analysis, X-ray diffraction, scanning electron microscopy, high-resolution transmission electron microscopy, and energy dispersive X-ray spectrometry were employed to characterize the chemical composition and structural features of the products. Well-crystallized elongated single-crystal Si nanofibers, coated with a thin SiO_2 amorphous layer, and crystallized carbon nanoparticles containing metals (e.g., Fe) and Si dominate. The highest yields of nanofibers and carbon particles were obtained from PTFE and Si-containing precursors, due to the volatility of SiF_4.

Introduction

Synthesis by thermolysis is one of the most promising innovations in materials science. Examples include ball bearings, nuclear safety shields, abrasives, high-temperature superconductors, and other technologically advanced items.[1] Metal−polytetrafluoroethene (M/PTFE) mixtures represent condensed systems in which vigorous exothermic reactions occur according to the idealized scheme

$$-(CF_2-CF_2)_n- + 4n\ M \rightarrow \downarrow 2n\ C + 4n\ MF$$

PTFE is chemically and thermally resistant due in part to the high energy of the C−F bond (481 kJ/mol). Nevertheless, fluorocarbon polymers can be used as oxidizing agents, since for many metals the metal−fluorine bond strength is even greater than that of the C−F bond. Thus, the M/PTFE mixtures are highly energetic heterogeneous materials in which the thermolysis rate is strongly dependent on the reactant particle size and the concentration of reducing agent in the mixture.[2−5] Because of the important advantages associated with M/PTFE reactions, such as a relatively high energy release, nonoxygen environment, low gas output, and the generation of multiphase reaction products, they are widely used, e.g., in IR flares, as igniters for solid fuel rocket engines, and in other pyrotechnics.[4,5] Syntheses are characterized by phase transitions in the forefront of thermolysis, heat release in a three phase flow field, time and space inhomogeneity of temperature fields, agglomeration and dispersion of the condensed phase formed, etc. The reaction is usually initiated by thermal decomposition of PTFE at ca. 770 K with evolution of volatile fluorine compounds, which react vigorously with a metal. Self-propagating heat waves, associated with the oxidation of metals at heating rates approaching 10^6 K s^{-1}, can yield new materials resulting from these ultrafast reactions.[6] Depending on the melting/boiling point of a respective metal, the process can run in a solid or liquid phase when the contact between the reactants is thereby increased. High thermolysis temperatures (e.g., theoretically exceeding 3000 K for Mg/PTFE composition[7]) and specific conditions for fast product growth with formation of elemental carbon, carbon compounds, and metal fluorides may thus favor the formation of novel nanostructures including nanocarbons. Strong IR emission during the thermolysis is thought to be related to, among other factors, hot carbon particles.[8] Hlavaty and Kavan[9] reported the preparation of polymeric carbon from a PTFE powder in a suspension of pure alkali metals in different organic solvents. Side reactions yielded highly reactive polyynes $(-C\equiv C-)_n$, which pose the fundamental question regarding the feasibility of preparing carbyne by defluorinating fluorinated polymers. Zhang et al.[10] studied the decomposition of PTFE by grinding with strontium oxide. In addition to the evolution of CO, amorphous carbon was formed during this process. Highly porous carbon with a carbynelike structure was prepared by defluorinating PTFE with lithium.[11] The product showed a higher heat capacity than activated carbon fiber, with almost the same Brunauer−Emmett−Teller surface area. In a comprehensive paper containing more than 400 references, Kavan[12] reviewed the electrochemical production of elemental carbon from suitable precursors, by either anodic oxidation (e.g., of hydrocarbons) or cathodic reduction (e.g., of carbon oxides or halides). Carbon chains and nanoparticles were also obtained by cathodic defluorination of perfluorinated hydrocarbons.[13] Raman spectra of the products revealed the presence of carbon chains (oligoynes) in addition to graphitelike carbon. Transmission electron microscopy (TEM) images showed that these carbons contain ca. 1% of nanotubes and carbon anions, in addition to a small (≈0.01%) quantity of fullerene C_{60}.

* To whom correspondence should be addressed. E-mail: ahuczko@chem.uw.edu.pl.
† Warsaw University.
‡ Military University of Technology.
§ University of Sussex.

10.1021/jp022183c CCC: $25.00
Published on Web 02/25/2003

Thermolysis is a quick and energy efficient way to prepare valuable materials. During the course of reaction, rapid solidification generates structures that would be unstable under normal conditions. This capability makes it possible to create materials that are otherwise difficult to make, such as elongated one-dimensional (1D) nanostructures. In the present study, we describe defluorination of PTFE with various metals or their alloys in a highly heterogeneous condensed system. The composition and morphology of the solid products formed under these specific conditions were studied.

Experimental Section

Thermolysis was carried out under an Ar (0.5 MPa) atmosphere in a calorimetric bomb[6] in order to monitor the heat of reaction. The instrument was calibrated by burning standard samples of benzoic acid in purified oxygen. The starting two component mixtures were prepared in the form of a 2 cm diameter pellet (5 g) made from fine powders (particle size below 100 μm) compressed at 10 MPa, i.e., at high density in order to efficiently dissipate the heat of reaction and to reduce the occurrence of "hot spots", which cause nonuniformity in the microstructure of the final product. The reactants were placed in a graphite crucible and ignited by an electrically heated thermolysis promoter attached to the top of the pellet. The main reaction time was 15−20 min, with ca. 10 min heating and subsequent cooling periods. At least two runs were performed for each mixture.

Differential thermal analysis (DTA)/thermogravimetric (TG) measurements for reactants (M50/PTFE50) were made using a MOM Budapest Derivatograph-PC under a nitrogen atmosphere and at a heating rate equal to 10 K/min.[6] The samples were compressed to form 20 mg pellets.

The heating rate across the whole combustion wave was evaluated from the increase of temperature measured by using K type thermocouple (0.06 mm wire, OMEGA Engineering, U.S.A.) with uncovered junction, embedded in a pressed sample. The thermoelectric power was measured using a digital voltmeter with the sampling frequency equal to 100 Hz. The measured results were summarized according to the spline function method.

The elemental analyses (Perkin-Elmer Analyzer CHNS/0 model 2400) of recovered solid products were carried out in order to determine the total carbon content. X-ray diffraction (XRD) spectra were measured using a Siemens Diffractometer D500 in conjunction with Cu Kα radiation. The XRD data were calculated, and the phase analysis was performed utilizing an in-house program, XRAYAN.

Solid reaction products were examined by scanning electron microscopy (SEM, Leo 5000, operating at 20 keV). The sample was also subjected to ultrasound treatment in acetone for 30 min and then transferred to a Cu grid coated with a holey carbon film for TEM investigations (H-7100, operating at 100 keV, and CM200 with an energy dispersive X-ray spectrometry (EDX) equipment attachment, operating at 200 keV).

Results and Discussion

Calorimetric Measurements. The ignition and reactants transformation occur when initial local increases in temperature are sufficient to initiate oxidation of the reductant and propagate a heat wave as more heat is released during the highly exothermic reaction. The heat release accompanying the process was measured for different M/PTFE mixtures as a function of the metal content. The initial concentration of components corresponded to the stoichiometric composition with the formation of metal fluorides and carbon. The calorimetric measurements (Figure 1) showed that the thermolysis proceeds in a self-sustaining high-temperature regime. The heats of the reaction range from very low (less than 1000 kJ/kg) for Zn/PTFE mixtures rich in metal to very high (more than 8000 kJ/kg) for the reactants containing Al_3Mg_4 at a concentration close to the postulated stoichiometry. Nevertheless, these numbers account for only ca. 70% of the theoretical exothermal effect calculated assuming the chemical equilibrium of the thermolysis.[7] Despite the incompleteness of the thermolysis, most of the mixtures are characterized by a comparatively wide concentration range of thermolysis reductants, from 15% to more than 90%, with the maximum heat release for stoichiometric compositions. Generally, the maximum heat release does not coincide with the postulated stoichiometry but occurs at somewhat higher reductant content. Whereas for Al_3Mg_4 it can be related to the surface oxidation of the alloy under consideration, such a justification no longer holds for ZrTi and FeSi alloys, which contain a quite high metal content. However, the melting points of the alloys exceed significantly the decomposition temperature of PTFE. Thus, diffusion occurs, which is facilitated by higher reductant content.

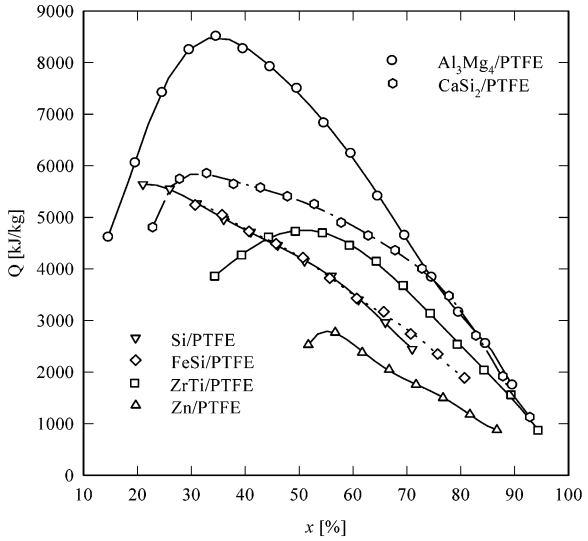

Figure 1. Heats of reaction for M/PTFE mixtures as a function of metal (M) content.

DTA/TG Measurements. The main stage of PTFE decomposition took place between 780 and 880 K. The exothermic reactions commence below 780 K for compositions containing Al_3Mg_4, Zn, $CaSi_2$, and FeSi when the reactants are still in a condensed phase. The first two are liquids at temperatures (melting endotherms between 720 and 750 K and 690−700 K for Al_3Mg_4 and Zn, respectively) that facilitate their reactions with PTFE. Therefore, the respective exothermal effects for these processes are large. No preignition heat release occurs for mixtures containing ZrTi or Si with PTFE, and DTA reveals the onset of ignition for these mixtures coincident with mass loss. This implies that the exothermic reactions begin after decomposition of PTFE. The thermolysis is especially violent for the ZrTi/PTFE mixture as shown by the sharp exothermal effect on the DTA curve and a very high rate of weight loss. Full decomposition is achieved at the lowest temperature (815 K) in this case, whereas for other reductants the temperature exceeds 860 K. When the black, fibrous product of $CaSi_2$/PTFE thermolysis was subsequently heated in air at 10 K/min, the white product exhibited a fibrous morphology. The chemical transformations were followed by monitoring the DTA/TG curves (Figure 2). A slightly exothermic oxidation begins at

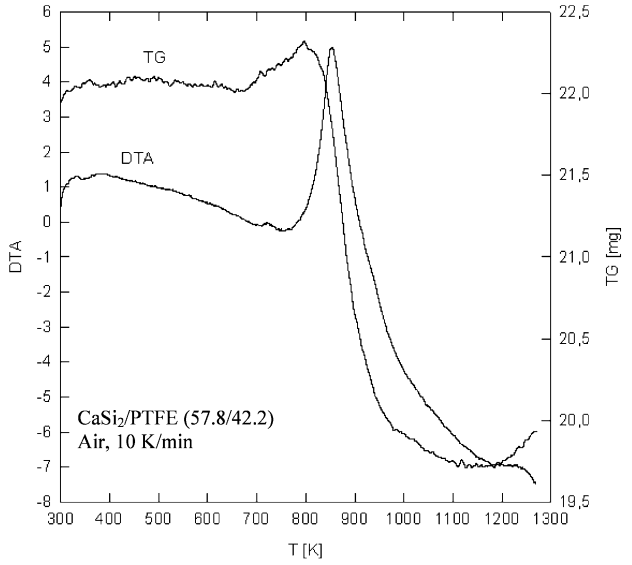

Figure 2. DTA/TG curves for the oxidation of products of $CaSi_2$/PTFE thermolysis.

670 K with the mass increase reaching 2.7 wt % at 800 K. At ca. 760 K, another strongly exothermal process commences with the distinctive mass decrease compromised by the mass gain related to the oxidation occurring in parallel. This mass loss ends at ca. 1110 K, the total being close to 12 wt %. The highest rate of mass decrease occurs at ca. 850 K in line with the maximum heat release. The temperature range for mass decrease, accompanied by the disappearance of the black materials, may suggest oxidation of free carbon present in the product, estimated to be 12 wt %. The slight mass increase, observed at lower temperature, may be related to the oxidation of Ca, which may still be present (as unreacted starting material) in the products since the reacting mixture was enriched in $CaSi_2$. Oxidation of Si can definitely be excluded in this temperature range.

Temperature and Heating Rate Measurements. The results of temperature measurements are shown in Figure 3a; Figure 3b illustrates time derivatives of the temperature profiles. The highest temperatures (close to 1800 K) were obtained for mixtures of PTFE with Al_3Mg_4 or $CaSi_2$, while the highest heating rate (almost 2×10^4 K s^{-1}) was obtained for the composition containing $CaSi_2$. Much lower temperatures (below 1500 K) and heating rates (even 1 order of magnitude!) were obtained for other mixtures, including the ones containing Si. A slower thermolysis, clearly visible for FeSi- and Zn-containing compositions, was observed ca. 780 K. It can be related to the endothermic processes of PTFE depolymerization and gasification.

Elemental and XRD Analyses. The results of both analyses, together with the initial compositions of the reactants, are presented in Table 1. The tests were carried out both with stoichiometric mixtures and with different $CaSi_2$ content for $CaSi_2$/PTFE compositions, since the latter mixtures showed the most interesting reaction history. The selected products were heated further in a quartz crucible for 1 h at 880−900 K in air to remove free carbon. Examples of XRD diffractograms are shown in Figure 4. Depending on the starting reactants, the carbon content of the solid products varied between 10 and 80 wt %. The higher carbon content was obtained for mixtures containing Si, i.e., for pure Si/PTFE, the carbon concentration was 82.3 wt %. This enrichment of the product with carbon can be related to the lower content of the other product (volatile metal fluoride), which, in the case of Si-containing mixtures, is gaseous SiF_4. For $CaSi_2$/PTFE, one can estimate (Figure 2 and Table 1) that elemental carbon accounts for almost 50% of the total. Calcination of the product resulted in a distinct decrease of carbon content (between 50 and 70%) due to its oxidation. The residual carbon can be related to carbide phases

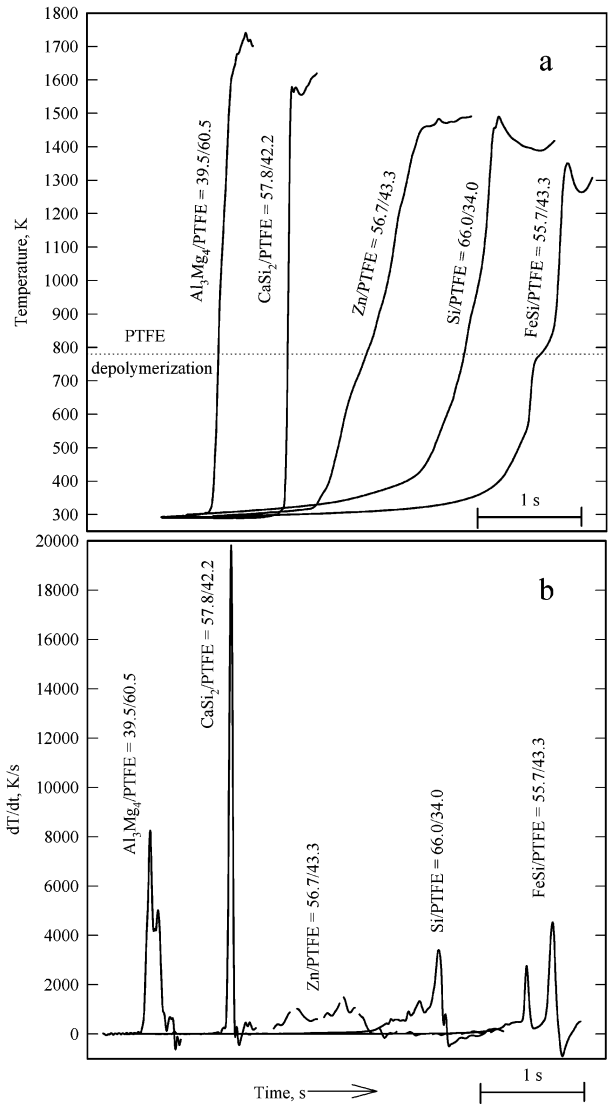

Figure 3. Temperature histories (a) and heating rates (b) during the thermolysis.

TABLE 1: Elemental and XRD Analyses

reactant composition	C (wt %)	H (wt %)	phases identified (XRD analysis)	C intensity (XRD analysis)
Zn (56.7)/PTFE (43.3)	10.7		ZnF_4	weak
Al_3Mg_4 (34.5)/PTFE (65.5)	17.1		MgF_2, Al, AlF_3, Al_4C_3	medium
ZrTi (49.3)/PTFE (50.7)	13.8		ZrF_4, TiF_3	weak
Cr (56.7)/PTFE (43.3)	11.8		CrF_2, CrF_3	weak
B (22.6)/PTFE (77.4)	58.9	0.9	B_4C, $B_{13}C_2$	strong
B (22.6)/PTFE (77.4)[a]	28.1	0.4	B_4C, $B_{13}C_2$	
Si (26.0)/PTFE (74.0)	79.6	0.2	Si, SiC	strong
Si (26.0)/PTFE (74.0)[a]	26.1	0.4	Si, SiC	
FeSi (35.7)/PTFE (64.3)	44.2		Si, Fe_3Si, Fe_5Si_3, SiC	strong
$CaSi_2$ (22.8)/PTFE (77.2)	43.3		Si, CaF_2, SiC	strong
$CaSi_2$ (27.8)/PTFE (72.2)	42.2		Si, CaF_2, SiC	strong
$CaSi_2$ (37.8)/PTFE (62.2)	32.1		Si, CaF_2, SiC	medium
$CaSi_2$ (47.8)/PTFE (52.2)	25.5		Si, CaF_2, SiC	medium
$CaSi_2$ (57.8)/PTFE (42.2)	22.1		Si, CaF_2, SiC	medium
$CaSi_2$ (57.8)/PTFE (42.2)[a]	8.8		Si, CaF_2, SiC	

[a] Product calcinated in air.

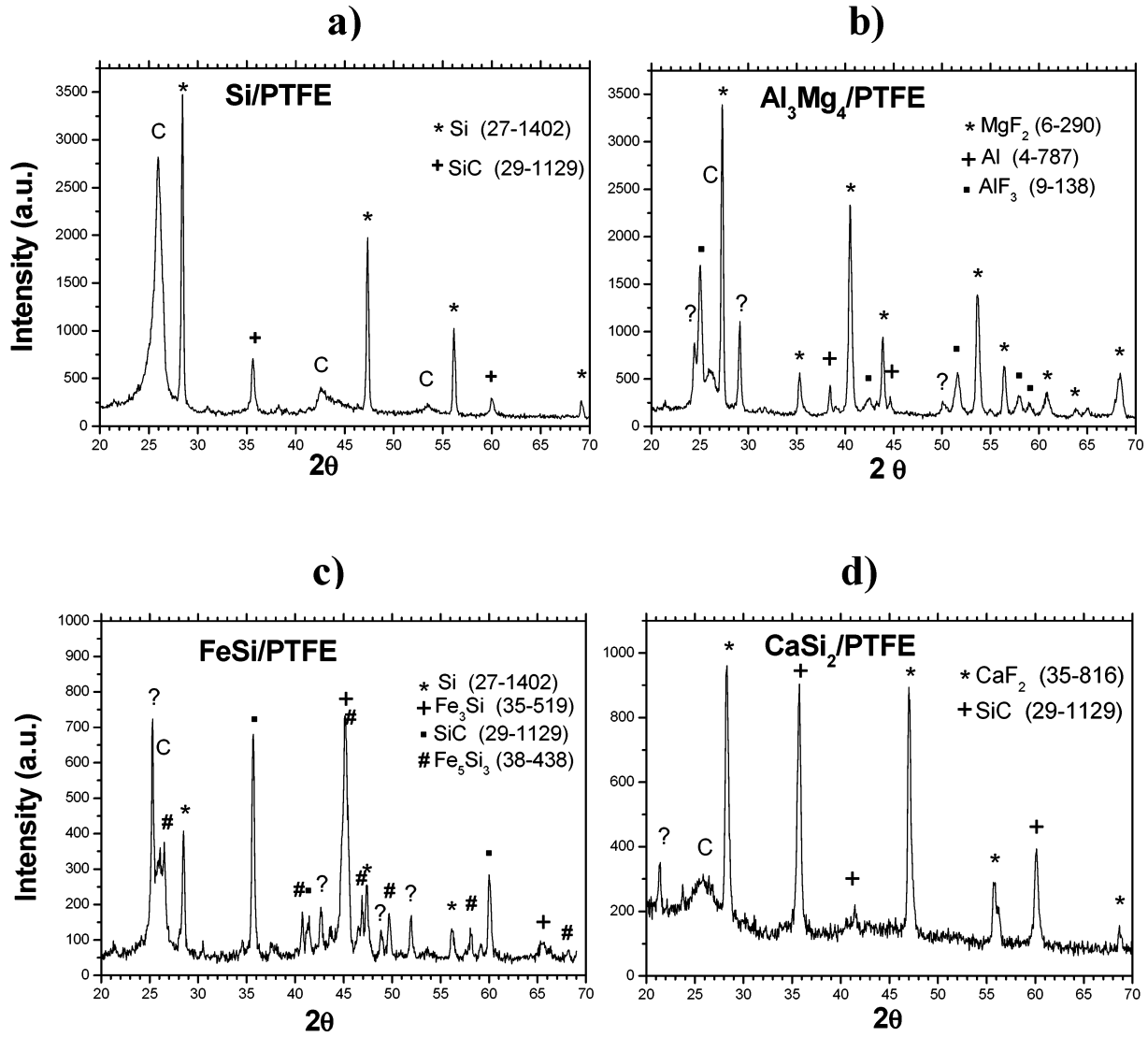

Figure 4. XRD spectra of products resulting from M/PTFE thermolysis. (a) Si/PTFE; (b) Al_3Mg_4/PTFE; (c) FeSi/PTFE; and (d) $CaSi_2$/PTFE.

due to its resistance against oxidation at the heating temperature. Different crystalline materials, including unreacted reductants, carbides, fluorides, and silicides, were detected by XRD. Some unidentified crystalline phases were also detected. The graphitelike carbon phase (turbostratic graphite) was identified in all products with the strongest peak (002) at 2θ in the 26.50−26.65° range. Both crystalline graphite and turbostratic carbon were detected in the product resulting from the thermolysis of the $CaSi_2$/PTFE mixture with the lowest $CaSi_2$ content. The increase of reductant content in these mixtures resulted in the distinct decrease of carbon content, and the increase of SiC content in the product was due to higher transformation of reactants. Thus, the excess of Si not only totally assimilated the evolving fluorine and escaped the reaction zone as SiF_4 gas (thus increasing PTFE decomposition) but also formed SiC efficiently. Obviously, the unreacted Si content in the product increased as well. The highest content of turbostratic graphite was again found in an Si/PTFE product confirming the above conclusion (efficient formation of gaseous SiF_4).

SEM. During SEM observations, we detected various types of novel nanostructures, including uniform carbon nanoparticles, huge spherical metal microparticles, and 1D ceramic fibers. Nanofibers/nanowires were present in all samples; however, for those containing Si as a component of the starting materials (Si, FeSi, and $CaSi_2$ mixed with PTFE), the yield of nanofibers is significantly high. A typical morphology of these nanofibers is shown in Figure 5. The fibers are ca. 20−100 nm in diameter and up to 10 μm in length. The carbon particles (accumulated in Figure 5a; FeSi/PTFE) are uniform, ca. 30−40 nm in diameter. In Figure 5b ($CaSi_2$/PTFE), the fibers display slightly larger dimensions than in Figure 5a; ca. 20−100 nm diameter and up to 20 μm in length, containing additional huge spherical particles, 1−1.5 μm in diameter. The nanofibers eventually produced by the latter three samples are different: $CaSi_2$/PTFE formed more, whereas Si/PTFE generated less. SEM observations also confirmed the conclusions from elemental and XRD analyses. With the increasing content of CaF_2 in reacting compositions (Figure 6), a distinct decrease of carbon and increase of nanofibers were observed.

TEM. TEM examinations revealed further detailed structural features of the thermolysis samples. The dimensions of these nanofibers are identical to those observed by SEM. Si-containing precursors resulted in more nanofibers (Figure 7a; FeSi/PTFE), and the other precursors led mainly to carbon particles (Figure 7b). However, these carbon particles appeared to be significantly different from those produced by the standard arc discharge process. They appear to be spherical at lower magnification, with a large hollow core. EDX examinations have detected the presence of associated metals and the Si signal in some cases. Other spherical metal particles are also present in most of the

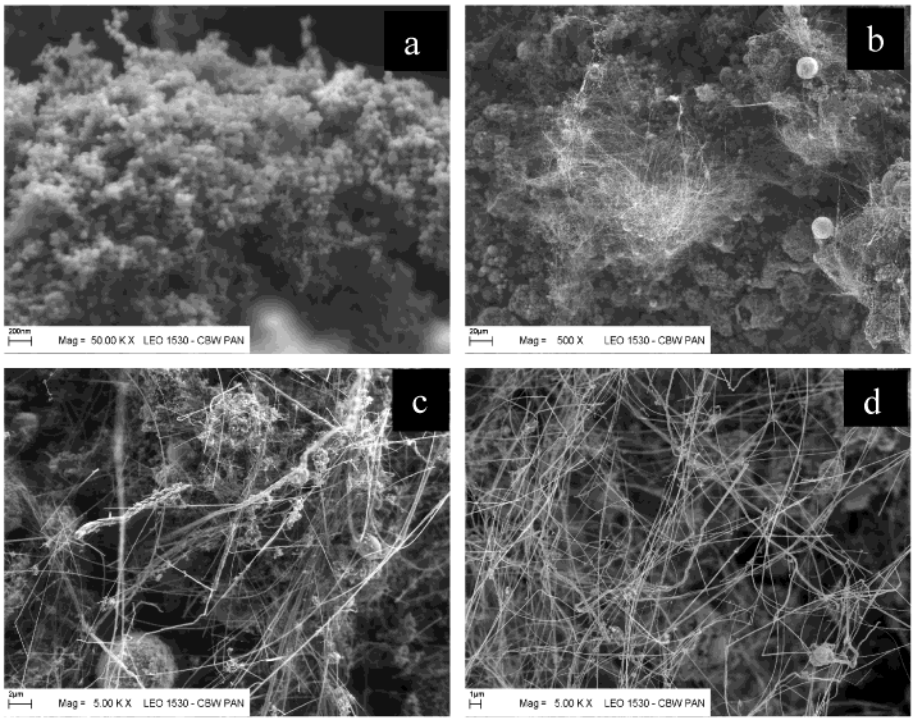

Figure 5. SEM images: (a) nanofibers and the accumulated carbon nanoparticles from the FeSi/PTFE sample; (b) larger nanofibers and metal particles from $CaSi_2$/PTFE.

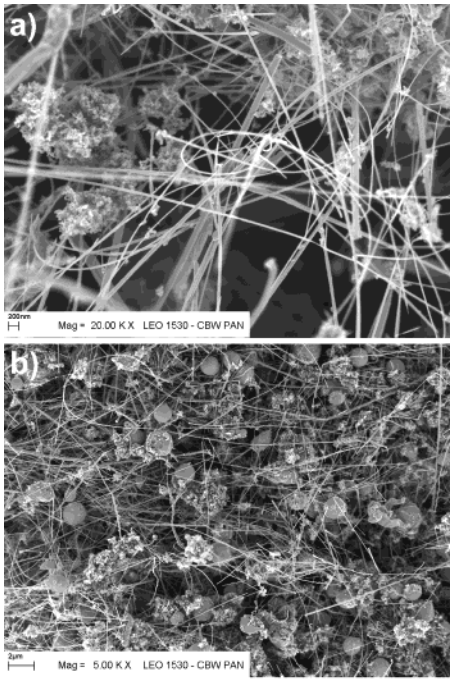

Figure 6. SEM images: (a) $CaSi_2$/PTFE (22.8/77.2) sample; (b) $CaSi_2$/PTFE (27.8/72.2) sample; (c) $CaSi_2$/PTFE (37.8/62.2) sample; (d) $CaSi_2$/PTFE (57.8/42.2) sample.

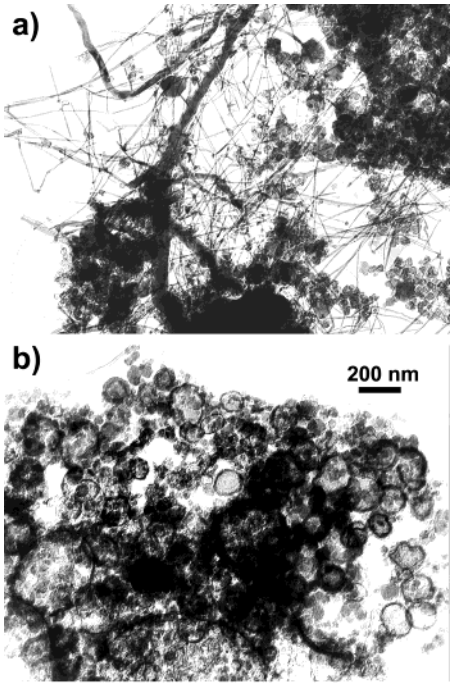

Figure 7. TEM images: (a) Si-containing precursors resulting mainly in nanofibers; (b) typical hollow carbon particles.

samples, although their diameters vary dramatically depending on the sample: from 20 nm to a few micrometers. In most cases, we observed metal particles attached to the fiber tip. Further high-resolution (HRTEM) observations showed that the hollow carbon particles (ca. 20−100 nm in diameter) consisted of crystallized layers, although severe layer defects were often observed (Figure 8a). This appeared to be a common feature for all samples. Taking into account the EDX observation that other metals or Si have often been found within these carbon particles, we suggest that these impurities could be the main reason for these layer defects. The nanowires from Si-containing precursors also exhibited similar structural characteristics, namely, well-crystallized, elongated single-crystal 1D Si nanowires, coated with an amorphous SiO_2 layer, a few nanometers thick as verified by EDX analysis (Figure 8b). The particle types attached to the fiber tips, associated with the precursors, seem to be of no significance. This demonstrates that the reaction temperatures (determined by heat release) play the key role in fiber growth.

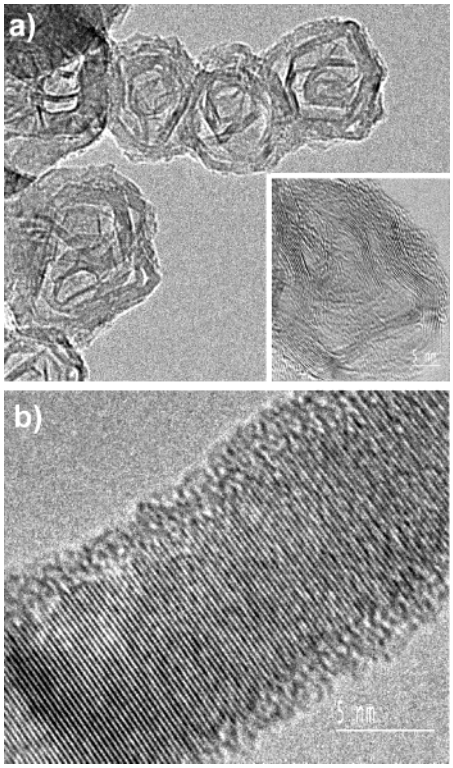

Figure 8. HRTEM images: (a) carbon nanoparticles (insert showing the layer defects of the particles); (b) elongated well-crystallized 1D Si nanowires from all Si-containing samples.

Conclusion

In summary, we have demonstrated that thermolysis offers great potential for generating 1D inorganic and carbon nanostructures. The exothermal reactions start at relatively high temperature, and the mixtures must have reached such temperatures at the input heat necessary for "ignition". However, local temperatures must be much higher for the extensive transformation to occur. This transformation into completely new morphology requires bond breakage and rearrangements of several different atoms within milliseconds. The thermolysis can be applied to various solid/liquid mixtures, particularly to M/PTFE systems. The advantages of this single-step approach include (i) self-sustaining reaction without extra heat consumption; (ii) relatively high process selectivity; (iii) high product formation rate; and (iv) simple equipment. Carbon nanoparticles, akin to those produced by arc discharge but with larger hollow cores, have been generated successfully in all samples in high yield. Well-crystallized elongated single-crystal Si nanofibers, sheathed with an amorphous SiO_2 layer, have also been produced in all Si-containing precursors in high yield.

Heat confinement in nanostructures can thus lead to drastic structural reconstruction and induces ignition under conditions not anticipated for bulk materials. Mechanistic and kinetic aspects of the thermolysis call for a more detailed study, which is in progress.

Acknowledgment. This work was supported by the Committee for Scientific Research (KBN) through the Department of Chemistry, Warsaw University, under Grant No. 7 T09A 020 20. We also thank the EPSRC for financial support.

References and Notes

(1) Varma, A.; Rogachev, S.; Mukasyan, A. S.; Hwang, S. *Adv. Chem. Eng.* **1998**, *24*, 79.
(2) Kubota, N.; Serizawa, C. *Propellants, Explos., Pyrotech.* **1987**, *12*, 145.
(3) Kuwahara, T.; Matsuo, S.; Shinozaki, N. *Propellants, Explos., Pyrotech.* **1997**, *22*, 198.
(4) Gocmez, A.; Yilmaz, A. G.; Pekel, F. *Propellants, Explos., Pyrotech.* **1999**, *24*, 65.
(5) Koch, E.-C.; Dochnahl, A. *Propellants, Explos., Pyrotech.* **2000**, *25*, 37.
(6) Huczko, A.; Lange, H.; Chojecki, G.; Cudziło, S.; Zhu, Y. Q.; Walton, D. R. M.; Kroto, H. W.; Presz, A.; Diduszko, R. *XVIth International Winterschool on Electronic Properties of Novel Materials "Molecular Nanostructures"*; Kirchberg, Austria; March 2−9, 2002, Abstr. Book, p 50.
(7) Cudziło, S.; Trzciłski, A. W. *Pol. J. Appl. Chem*. **2001**, *26*, 25.
(8) Koch, E.-C. *Propellants, Explos., Pyrotech.* **2001**, *26*, 3.
(9) Hlavaty, J.; Kavan, L. *Carbon* **1999**, *37*, 1029.
(10) Zhang, Q.; Matsumoto, H.; Saito, F. *Chem. Lett.* **2001**, 148.
(11) Soshi, S.; Hideyuki, K.; Hiroki, T.; Asao, O.; Yasushi, S.; Yoshio, Y. *Electrochem. Solid-State Lett.* **2001**, *41*, A5.
(12) Kavan, L. *Chem. Rev.* **1997**, *97*, 3061.
(13) Kavan, L. In *Electronic Properties of Novel Materials−Science and Technology of Molecular Nanostructures*; Kuzmany, H., Fink, J., Mehring, M., Roth, S., Eds.; AIP Conference Proceedings: 1999; Vol. 486, p 209.